Atmospheric Retrieval of Exoplanets

Nikku Madhusudhan

Abstract Exoplanetary atmospheric retrieval refers to the inference of atmospheric properties of an exoplanet given an observed spectrum. The atmospheric properties include the chemical compositions, temperature profiles, clouds/hazes, and energy circulation. These properties, in turn, can provide key insights into the atmospheric physicochemical processes of exoplanets as well as their formation mechanisms. Major advancements in atmospheric retrieval have been made in the last decade, thanks to a combination of state-of-the-art spectroscopic observations and advanced atmospheric modeling and statistical inference methods. These developments have already resulted in key constraints on the atmospheric H_2O abundances, temperature profiles, and other properties for several exoplanets. Upcoming facilities such as the JWST will further advance this area. The present chapter is a pedagogical review of this exciting frontier of exoplanetary science. The principles of atmospheric retrievals of exoplanets are discussed in detail, including parametric models and statistical inference methods, along with a review of key results in the field. Some of the main challenges in retrievals with current observations are discussed along with new directions and the future landscape.

Introduction

A spectrum of an exoplanet provides a window into its atmosphere. A spectrum encodes information regarding the various interconnected physicochemical processes and properties of the atmosphere which are revealed through their influence on the radiation emerging through the atmosphere before reaching the observer. These properties include the chemical composition, temperature structure, atmospheric circulation, clouds/hazes, all of which leave their imprints on the spectrum. Given an observed spectrum, the challenge is to disentangle these various components. This

Institute of Astronomy, University of Cambridge, Madingley Road, Cambridge CB3 0HA, UK
e-mail: nmadhu@ast.cam.ac.uk

is the goal of 'atmospheric retrieval' – to retrieve the atmospheric properties of an exoplanet from an observed spectrum. The retrieved properties can in turn provide insights into the various atmospheric physical and chemical processes as well as into their formation history. While the introduction of atmospheric retrieval methods to exoplanetary science is a relatively recent and independent development (Madhusudhan and Seager 2009; Madhusudhan et al. 2011a), alternate techniques have been in wide usage in the context of Earth-based remote sensing (Rodgers 2000) and retrievals of solar system planets (Irwin et al. 2008).

What differentiates exoplanetary atmospheric retrieval from solar system applications is the uniquely challenging nature of observing exoplanetary atmospheres. Firstly, unlike solar system planets, observed exoplanetary spectra are inherently disk-averaged over the spatially unresolved planet. Secondly, given their astronomical origins well beyond the solar system, exoplanetary spectra are naturally substantially fainter, and hence of much lower signal-to-noise (SNR), compared to solar-system objects. Thirdly, any complementary in situ measurements or a priori knowledge possible in the solar system are unavailable for exoplanetary atmospheres. Finally, the parameter space of exoplanetary atmospheres is substantially wider than that of solar system planets. For example, while the equilibrium temperatures of most solar system planets lie below 300 K those of exoplanets extend up to $\sim$3000 K. Similarly large ranges are natural in all other atmospheric parameters and processes - gravities, chemical compositions, circulation patterns, degree and type of insolation, etc, implying enormous complexity and diversity in exoplanetary atmospheres far beyond those experienced in the solar system. The combination of these various factors make exoplanetary atmospheres enormously more challenging to study compared to those of solar system objects, and necessitate substantially more robust techniques for atmospheric modeling and retrieval to make the best use of the limited spectral data available.

The origins of atmospheric retrieval techniques for exoplanets were motivated by the 'degeneracy problem' faced by early atmospheric observations. Initial molecular detections were claimed based on few channels of infrared photometry or low-resolution spectrophotometry with low SNR (e.g. Barman 2007; Tinetti et al. 2007; Grillmair et al. 2008; Swain et al. 2008, albeit some of these datasets have since been revised substantially), such that the spectral features were rarely discernible to the eye. Similarly, temperature inversions were claimed in hot Jupiters based on broadband photometric observations (e.g Knutson et al. 2008, 2009; Burrows et al. 2007, 2008). These inferences were made using a limited set of forward models containing the putative molecules and assumed temperature profiles that qualitatively matched the data. While the number of free parameters in the forward models typically far exceeded the number of data points then available, the number of models compared against the data were rather limited. This approach left vast areas of parameter space unexplored and degeneracies between various model parameters unknown, thereby providing little statistical basis to the claimed detections. The desire to provide a statistically robust framework to derive atmospheric properties of exoplanets from such low resolution data gave birth to the idea of atmospheric retrieval for exoplanets (Madhusudhan and Seager 2009). Atmospheric retrieval techniques have since

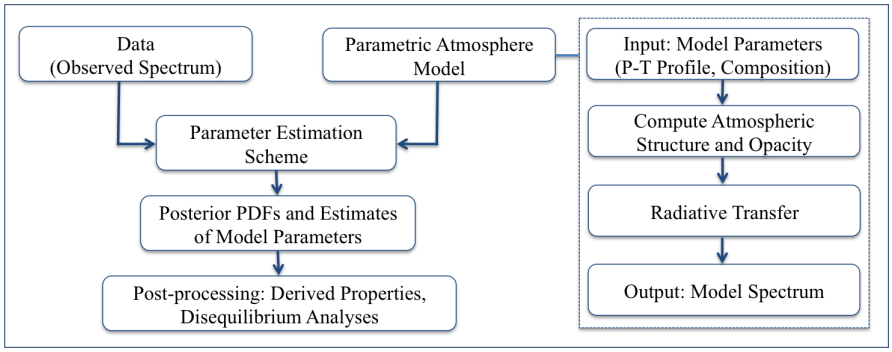

Fig. 1 Schematic of atmospheric retrieval. Given an observed spectrum and a parametric model of a planetary atmosphere, a parameter estimation method is used to derive the model parameters. The components of a typical atmospheric model are shown on the right. The free parameters typically correspond to the pressure-temperature (P-T) profile and the composition, including the chemical abundances and cloud/haze properties, depending on the datasets. The statistical inference and parameter estimation methods used in contemporary retrieval codes typically allow computation of full posterior probability density functions (PDFs) of the model parameters given a data set, a typical output shown in Fig. 2. These PDFs can also be used to compute PDFs of derived quantities such as elemental abundance ratios from those of molecular abundances. In recent advancements retrieval codes are also being coupled with self-consistent equilibrium models to place constraints on departures from radiative-convective and chemical equilibria (Gandhi and Madhusudhan 2018).

advanced greatly in tandem with parallel advancements in atmospheric observations of exoplanets.

In the present chapter we present a pedagogical review of exoplanetary atmospheric retrieval. We first present an overview of the key principles of atmospheric retrieval. We then discuss two primary components of retrieval methods, namely, parametric forward models and statistical inference methods. We then discuss key results in the field from retrievals of state-of-the-art observations. We conclude with a discussion of key issues in this area and the future landscape.

Overview of Atmospheric Retrieval

In its simplest form, 'retrieval' is synonymous with fitting an atmospheric model to an observed spectrum and estimating the model parameters along with uncertainties. A schematic of atmospheric retrieval for exoplanets is shown in Fig. 1 with an example output in Fig. 2, and a list of extant retrieval codes in the literature is shown in Table 1. A parameter estimation problem requires three key components:

1. A reliable data set, in the present case an atmospheric spectrum.
2. An accurate model, in the present case a parametric atmosphere model.
3. A suitable parameter estimation method.

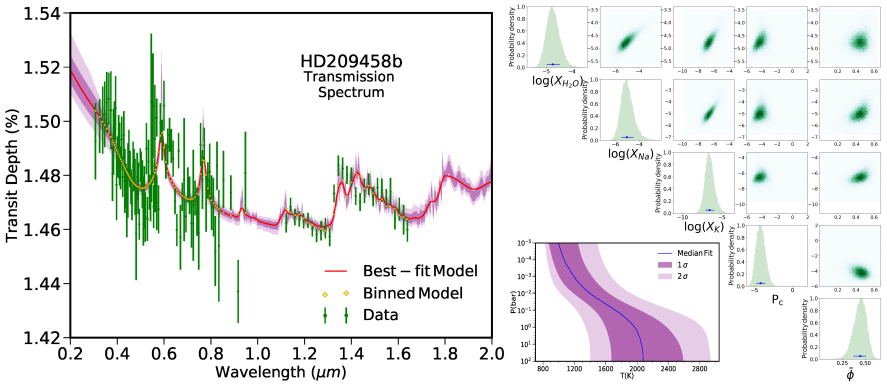

Fig. 2 Example of atmospheric retrieval for a transmission spectrum of the hot Jupiter HD 209458b. The left panel shows an observed spectrum in green along with the model fit and significance contours in purple. The right panel shows the posterior probability distributions of the retrieved compositions and the retrieved pressure-temperature profile.

All these components started becoming accessible for studying exoplanetary atmospheres only about a decade ago. The history of exoplanetary atmospheric retrieval is essentially the history of key developments in each of these aspects. In this section, we discuss the basic principles of atmospheric retrieval for exoplanetary atmospheres.

Self-consistent models vs parametric retrieval models

At the outset it is important to distinguish between the two paradigms for forward modeling of spectra of exoplanetary atmospheres - self-consistent models and parametric models used for atmospheric retrieval. Self-consistent models refer to models where the physicochemical properties and processes of the atmosphere are assumed to be known a priori. For example, a one-dimensional equilibrium model to compute thermal emission from a planet typically assumes a plane parallel atmosphere under the constraints of hydrostatic equilibrium, chemical equilibrium, local thermodynamic equilibrium (LTE), and radiative-convective equilibrium. The inputs to such a model are typically the system properties, or 'fixed parameters', such as the planetary bulk properties (e.g. mass, radius, and/or gravity), orbital properties (e.g. separation), and the spectrum of the host star irradiating the planet. Such a model also assumes an elemental composition of the planetary atmosphere, apart from other ancillary parameters (e.g. day-night energy redistribution efficiency, presence of clouds, etc.). Given these input parameters and the equilibrium assumptions such a model computes the radiative transfer in the atmosphere to generate an output spectrum for the desired viewing geometry. Self-consistent models span a wide range of complexity depending on the applications, ranging from 1D equilibrium

models to 3D General Circulation Models (GCMs) as well as models with non-equilibrium chemistry with varying levels of detail. A more detailed description of self-consistent models can be found in a number of recent sources(e.g. Burrows et al. 2008; Fortney et al. 2008; Heng and Marley 2017; Gandhi and Madhusudhan 2017).

While self-consistent models are invaluable for investigating detailed atmospheric processes under controlled conditions they are limited in their capability to robustly interpret observed spectra. Firstly, self-consistent models, by definition, assume that the physics and chemical compositions underlying the atmospheric processes are known. On the contrary, the novelty and diversity of exoplanetary atmospheres means that very little is known about them a priori and that the atmospheres could diverge substantially from the self-consistent model assumptions. Secondly, self-consistent models are not amenable to detailed parameter estimation methods due to their long computation times. For example, given the intricate degeneracies between the various atmospheric properties a typical model fitting to a spectral dataset could involve 10^5 - 10^6 model evaluations, which are prohibitive even for the simplest of self-consistent models, e.g. 1-D equilibrium models. The desired solution to interpret observed spectra of exoplanetary atmospheres is therefore a modeling paradigm which allows for (a) fast model evaluations, and (b) a parametrization of atmospheric properties that captures properties of self-consistent models as well as possible deviations thereof. For example, such a model should be able to replicate the temperature profiles, compositions, and spectra of self-consistent models for the same system parameters but also be flexible enough to model profiles and compositions that are not in equilibrium.

Retrieval methods, on the other hand, employ parametric forward models to extract the atmospheric properties from observed spectra. An inspection of a nominal cloud-free self-consistent model reveals that the atmospheric spectrum is governed mainly by the pressure-temperature (P-T) profile and the chemical composition of the atmosphere, both of which are calculated self-consistently under equilibrium conditions in such models, with the additional possibility of clouds. As such self-consistent models have no free parameters but only fixed parameters. The key idea in retrieval models is to use parametric forms for the P-T profile and the composition, which leads to two key advantages. Firstly, computing the P-T profile and chemical compositions are the most time consuming steps in self-consistent models. Therefore, parameterizing both these properties substantially shortens the computing time of a model. Secondly, there is no longer the need to assume equilibrium conditions because the P-T profile and chemical compositions are estimated directly from the data. These parametric models can be coupled with statistical parameter estimation methods to efficiently explore the model parameter space thereby allowing to formally fit the models to a given dataset and estimate the P-T profiles, compositions, and other parameters, e.g. clouds/hazes, etc. This functionality is the backbone of atmospheric retrieval.

An atmospheric retrieval code has two components: 1. a parametric model to compute the atmospheric spectrum for given atmospheric parameters, 2. an optimization algorithm, i.e., a statistical inference method to sample the model parame-

ter space given the data. For a given dataset the optimization technique explores the model parameter space in search of models fitting the data and in the process creates posterior probability distributions of all the model parameters. In the following sections we discuss both these components in detail, followed by a review of results from retrievals in the literature.

Table 1 Exoplanetary Atmospheric Retrieval Codes

Code Name/Author[a]	Forward Model	Inference Method[b]	References
Madhusudhan & Seager	Primary Transit Secondary Eclipse	Grid Search	Madhusudhan and Seager (2009)
Madhusudhan et al	Primary Transit Secondary Eclipse	MCMC	Madhusudhan and Seager (2010) Madhusudhan et al. (2011a, 2014a)
CHIMERA	Primary Transit Secondary Eclipse Direct Imaging	OE, BMC, MCMC and Multinest NS	Line et al. (2013, 2014); Todorov et al. (2016)
NEMESIS	Primary Transit Secondary Eclipse	OE	Barstow et al. (2017) Lee et al. (2012)
Benneke & Seager	Primary Transit	Multinest NS	Benneke and Seager (2013)
$\mathscr{T}$-REx	Primary Transit Secondary Eclipse	Multinest NS, MCMC	Waldmann et al. (2015b,a)
HELIOS-R	Direct Imaging Secondary Eclipse	Multinest NS	Lavie et al. (2017) Oreshenko et al. (2017)
ATMO	Primary Transit Secondary Eclipse	MCMC	Wakeford et al. (2017); Evans et al. (2017)
BART	Primary Transit Secondary Eclipse	MCMC	Cubillos (2015) Blecic (2015)
POSEIDON	Primary Transit	Multinest NS	MacDonald and Madhusudhan (2017a)
HyDRA	Secondary Eclipse	Multinest NS	Gandhi and Madhusudhan (2018)

[a] Here we only list codes reported in published works that have been used on actual observations of exoplanetary spectra.

[b] The statistical inference and parameter estimation method used in the retrieval code, e.g., Markov chain Monte Carlo (MCMC), Bootstrap Monte Carlo (BMC), Optimal Estimation (OE), and Nested Sampling (Multinest NS). See text for discussion on the different methods.

Models for Atmospheric Retrieval

The forward models and their parametrization for retrieval depend on the nature of the atmospheric observations in question. Exoplanetary atmospheric spectra used for retrievals have been observed in primarily three configurations: (a) transmission spectra of transiting exoplanets, (b) emission spectra of transiting exoplanets, and (c) emission spectra of directly-imaged planets[1]. Depending on the observing mode and geometry the observed spectrum is sensitive to a certain region of the atmosphere thereby requiring the corresponding model set-up and free parameters as discussed below.

General Framework and Free Parameters

The goal of a parametric forward model used for retrievals is to compute a model atmospheric spectrum for the required observational configuration given the properties of the atmosphere as free parameters. So, there are two components to a forward model, as shown in Fig. 1: (1) computing the structure of the atmosphere, i.e. profiles of pressure (P), temperature (T), density (ρ), concentrations (f_i) of individual chemical species, cloud/haze profile, if any, etc., and (2) computing the radiative transfer for the given atmospheric structure. Here we briefly describe the general principles for computing the atmospheric structure. The radiative transfer for each observing configuration will be discussed in following subsections.

Common to all the models used in retrieval are some general assumptions about the atmospheric structure. The atmospheres are assumed to be generally spherically symmetric, in hydrostatic equilibrium, and in local thermodynamic equilibrium (LTE). The opacities for the radiative transfer are usually computed in a line-by-line manner (Madhusudhan and Seager 2009; Madhusudhan et al. 2014a; Line et al. 2013; Benneke and Seager 2013) but some codes use correlated-K opacities (Lee et al. 2012; Lavie et al. 2017). The P-T profile and chemical compositions are free parameters in the models. Given a P-T profile, the profiles of P, T, and ρ as a function of radial distance (r) are determined using the assumption of hydrostatic equilibrium and the ideal gas equation of state. Given the parametric chemical composition, the mean molecular weight and total number density (n) are also determined. Once all these quantities are determined, the remaining task is to determine the radiation field emerging from the system for the given geometry by considering the appropriate scheme for radiative transfer in the atmosphere.

The parameters for forward models used in retrievals correspond to three broad properties: chemical composition, P-T profile, and clouds/hazes. The chemical composition of the atmosphere is represented by the volume mixing ratios (f_i) of

[1] Recently, retrieval codes are also being built for reflection spectra of directly imaged planets that can be obtained with future space-based facilities (Lupu et al. 2016). However, we do not discuss these models here since they have so far only been used on simulated data and not on observed spectra of known exoplanets.

the species, e.g. number density of each species relative to the total number density, implying as many free parameters as the number of species (typically between 4 and 10). Usually, for H_2-rich species the prominent absorbers such as H_2O, CO, CH_4, CO_2, Na, K, etc., are included. Additionally, the mixing ratios are typically assumed to be uniform in the region of the atmosphere probed by the observations. The *P-T* profile is represented by one of two parametric *P-T* profiles used in the retrieval literature, either the 6-parameter profile prescribed by Madhusudhan and Seager (2009) or the 5-parameter profile reported by Guillot (2010) which, for example, was used in Line et al. (2013). Both profiles have been shown to reproduce characteristic *P-T* profiles in planetary atmospheres, though the first one offers more flexibility at the cost of an extra parameter (Line et al. 2016). Additionally, the model can include opacity due to the presence of clouds or hazes in the atmosphere as well as the possibility of inhomogeneous clouds (Benneke and Seager 2012; Kreidberg et al. 2015; Barstow et al. 2017; Line and Parmentier 2016; MacDonald and Madhusudhan 2017a), adding $\gtrsim 3$ more free parameters. In total, a typical parametric model has $\gtrsim$10 free parameters.

Transmission Spectra of Transiting Planets

A transmission spectrum is observed when a planet transits in front of the host star. In this geometry some light from the host star passes through the atmosphere at the day-night terminator region of the planet before reaching the observer. This light is subjected to extinction, i.e. absorption and/or scattering, in the planetary atmosphere. This modified stellar spectrum when subtracted from the original stellar spectrum obtained out of transit gives the extinction spectrum of the planetary atmosphere. A 'transmission spectrum' is represented as the extinction spectrum normalized by the original stellar spectrum and is essentially the transit depth as a function of the wavelength (Seager and Sasselov 2000; Seager 2010). The computation of a transmission spectrum at different levels of complexity, analytically and numerically, can be found in various works (Brown 2001; Hubbard et al. 2001; Seager and Sasselov 2000; Lecavelier Des Etangs et al. 2008; Miller-Ricci et al. 2009; Fortney et al. 2010; de Wit 2015; Bétrémieux and Kaltenegger 2015; MacDonald and Madhusudhan 2017a; Robinson 2017). Here we provide a brief outline.

In its simplest form the transmission spectrum can be expressed as

$$\Delta_\lambda = \left(\frac{R_{p,\lambda}}{R_{s,\lambda}}\right)^2 = \frac{2}{{R_s}^2}\int_0^{R_{max}} rdr\,(1-e^{-\tau_\lambda(r)}), \tag{1}$$

where λ is the wavelength, R_p and R_s are the planetary and stellar radii, respectively, and R_{max} is the maximum height of the observable atmosphere typically set at a reasonably high value. r is the impact parameter or height in the atmosphere perpendicular to the direction of the ray, and $\tau(r)$ is the slant optical depth through the chord traversed by a ray at the impact parameter r. The optical depth encoun-

tered by a ray as it traverses a chord is governed by the opacity from the planetary atmosphere at various pressures, temperatures, and chemical compositions on its path. The transmission spectrum is a cumulative effect of the opacity encountered by all the rays within the planetary atmosphere before reaching the observer.

Thermal Emission Spectra of Transiting Planets

The transit geometry allows observations of thermal emission from the dayside atmosphere of the planet at opposition, also known as secondary eclipse or occultation. The occultation depth gives the planet star flux ratio as

$$\frac{f_p}{f_s} = \frac{F_{out} - F_{in}}{F_{out}}, \tag{2}$$

where F_{out} and F_{in} are the fluxes from the system observed out of eclipse and during eclipse, respectively, and f_p and f_s are the planetary and stellar fluxes. The observed flux from a spherical body of radius R at a distance d is related to the specific intensity of radiation at its surface by $f_\lambda = \pi I_\lambda R^2/d^2$. Thermal emission models are used to compute the planetary spectrum given by $I_{\lambda,p}$ whereas the stellar spectrum is obtained from standard libraries of stellar models. The observation of f_p/f_s means that the distance to the system need not be known and, since the planetary radius is already know from transit, only $I_{\lambda,p}$ needs to be computed in models.

Models of thermal emission spectra used in retrievals generally assume a 1-D plane parallel geometry (e.g. Seager 2010; Madhusudhan and Seager 2009; Line et al. 2013). Consider a ray with spectral intensity $I_{0,\lambda}$ originating from a layer in the atmosphere at an optical depth τ with a direction cosine μ. The specific intensity of the ray as it emerges out from the top of the atmosphere is given by

$$I_\lambda(\tau,\mu) = I_{0,\lambda}(\tau,\mu)e^{-\tau_\lambda/\mu} - \frac{1}{\mu}\int_\tau^0 S_\lambda e^{-t/\mu}dt. \tag{3}$$

In this notation, $\tau = 0$ at the topmost layer of the atmosphere and increases inward such that $\tau \to \infty$ for the deepest layers. S_λ is the source function, which for an atmosphere in Local Thermodynamic Equilibrium (LTE) is the Planck function. A ray generated in a deeper layer of the atmosphere traverses through the layers above before escaping the atmosphere and reaching the observer. On its way out photons in the ray are absorbed or enhanced depending on the opacity and temperature profile in the atmosphere. For an atmosphere where the temperature decreases outward monotonically the layers above are always cooler than the layers below leading to absorption of the outgoing radiation. On the other hand, where temperature increases outward (a thermal inversion) the source function contributes additional flux to the outgoing ray thereby causing emission features. Furthermore, the degree of absorption or emission is critically influenced by the magnitude of the temperature gradient as well as the opacity of the atmosphere at the particular wavelength in

question. Therefore, emission spectra are strong probes of the *P-T* profile of the dayside atmosphere as well as the composition. The model parametrization is similar to that of transmission spectra, with the exception that all the quantities now correspond to the 1-D dayside-averaged properties of the atmosphere. More details on thermal emission models used in retrieval can be found in various studies (e.g., Madhusudhan and Seager 2009; Seager 2010; Line et al. 2013; Waldmann et al. 2015a; Lavie et al. 2017).

Directly Imaged Spectra

Models used in retrievals of spectra from directly imaged exoplanets are essentially the same as those of emission spectra for transiting planets discussed above. The only difference is in the observables and, hence, free parameters. For a directly imaged planet, only the planetary flux spectrum (f_p) is observed and essentially no other information about the planet is measured, including the mass and radius. As such, the planetary radius, gravity, and distance to the system are additional free parameters in the model along with the *P-T* profile, chemical composition, and cloud parameters, if any.

Statistical Inference and Parameter Estimation Methods

Central to atmospheric retrieval is the parameter estimation method used to retrieve the model parameters given an observed spectrum. As discussed in previous sections, atmospheric retrieval of exoplanets is complicated by various factors including the complexity of atmospheric models, strong degeneracies between the model parameters, lack of prior knowledge, and scarcity of the data. The goal of a desired optimization algorithm is to sample a high-dimensional (10+) parameter space extensively and efficiently in search of the model solution space given the data. In order to address these various challenges, the parameter estimation methods used for atmospheric retrieval have evolved greatly over the years as discussed below and shown in table 1.

From Grid-based Sampling to Bayesian Inference

Exoplanetary atmospheric retrieval has come a long way from grid-based sampling to detailed parameter estimation using Bayesian inference methods. The first instance of exoplanetary atmospheric retrievals (Madhusudhan and Seager 2009) explored a ten-dimensional (10-D) parameter space using a large grid of 10^7 models for each planet. Arguably, a grid of reasonable resolution in a 10-D parameter space

can exceed 10^{10} models, which made it computationally prohibitive even for parametric models. Therefore, empirical metrics were used to narrow down the search volume to a more amenable 10^7 models. This allowed computation of contours of a goodness-of-fit statistic, e.g. a reduced χ^2 , over the search volume and statistical constraints on the atmospheric parameters for a given dataset. This approach helps to obtain an empirical understanding of the model parameter space when developing a new parametric model and in conducting feasibility studies, such as limits on computational efficiency, search volume, etc. However, once a working model is established the exploration of the parameter space using such a method is both insufficient in the grid resolution and limiting in computational efficiency. Therefore, subsequent retrieval studies have investigated more formal parameter estimation methods for atmospheric retrieval while retaining the general model parametrization.

Bayesian inference methods have gained prominence in the last decade for parameter estimation in diverse areas of astronomy, from precision cosmology (e.g., Tegmark et al. 2006) to exoplanet detection (e.g., Ford 2005; Eastman et al. 2013). They allow evaluation of the full posterior distribution of the model parameters given a dataset, and prior knowledge, if any, by efficiently and comprehensively sampling the model space. Such methods are particularly useful in problems with high-dimensional and strongly degenerate parameter spaces, as is the case for exoplanetary atmospheres. Therefore, Bayesian inference methods have over the years become the mainstay of exoplanetary atmospheric retrieval codes. As shown in Table 1, retrieval codes have incorporated a range of Bayesian inference techniques spanning MCMC (Madhusudhan et al. 2011a; Benneke and Seager 2012; Line et al. 2013), Optimal Estimation (Lee et al. 2012; Line et al. 2012), and Nested Sampling (Benneke and Seager 2013; Waldmann et al. 2015b; Lavie et al. 2017; MacDonald and Madhusudhan 2017a; Gandhi and Madhusudhan 2018).

Bayesian Inference

A thorough exposition on Bayesian inference methods can be found in various sources (see e.g., Trotta 2017) and their applications to exoplanetary atmospheric retrievals in the above studies. In what follows, we briefly discuss some key aspects. The foundation of Bayesian inference lies in the eponymous Bayes theorem which in the current context can be written as follows.

$$p(\theta|d) = \frac{p(d|\theta)\ p(\theta)}{p(d)}. \tag{4}$$

Here, θ denotes the set of parameters of an atmospheric model and d denotes the data, such as an observed spectrum. $p(\theta|d)$ is the posterior probability distribution of the model parameters given the data. $p(d|\theta)$, known as the likelihood function ($\mathscr{L}$), is the probability of the data given a parameter set. $p(\theta)$ is the prior probability distribution (π) of the model parameters independent of the data. $p(d)$, referred

to as the evidence $\mathscr{Z}$, is the likelihood of the data marginalized over the parameter space. When considering a single model M, $\mathscr{Z}$ provides the normalization for the posterior. However, when considering multiple models $\{M_i\}$ with different parameterizations, the computations of $\mathscr{Z}_i$ allows model comparisons by considering the relative evidences between different models.

The goal in Bayesian inference is to determine the posterior distributions $p(\theta|d)$ of the model parameters for a given dataset and considering any prior knowledge of the parameters. The likelihood function ($\mathscr{L}$) determines the degree of model fit to the data for a given point in the model parameter space as

$$\mathscr{L} = \mathscr{L}_0 \exp(-\chi^2/2), \tag{5}$$

$$\text{where } \chi^2 = \sum_i (d_i - m_i)^2/\sigma_i^2. \tag{6}$$

Here d_i and σ_i denote the mean and standard deviation of the ith data point, and m_i is the corresponding model prediction for the given parameter set. The different Bayesian inference methods (e.g. MCMC versus Nested sampling) use different approaches to sample the model parameter space and to estimate the posterior distributions and evidences.

Optimal Estimation Method

The Optimal Estimation (OE) method has its roots in Earth-based remote sensing (Rodgers 2000) and in retrievals of planetary atmospheres in the solar system (Irwin et al. 2008). More recently, it has been applied to retrievals of exoplanetary atmospheres (Lee et al. 2012). The method involves optimizing the likelihood function using a non-linear least squares minimization scheme such as the Levenberg-Marquardt algorithm. The OE method allows specification of priors for the parameters in the cost function, assuming a Gaussian-distributed prior covariance matrix. This is particularly relevant for Earth based retrievals where prior values of parameters can be approximated based on direct measurements (Irwin et al. 2008). The advantage of this method is that only a small number of iterations are required to obtain a model fit to the spectral data and is known to converge efficiently when high resolution and high signal-to-noise (SNR) data are available, e.g., in spectral retrievals of Earth and solar system objects.

The OE method is somewhat limited for large and multi-modal parameter spaces with strong degeneracies and non-Gaussian posterior distributions, which is typically the case for exoplanetary atmospheres. The method has been shown to be inaccurate for low-resolution low-SNR data as common for current exoplanetary spectra (Line et al. 2013), but in the limit of high-resolution high-SNR data it approaches the performance of more sophisticated Bayesian methods discussed below for single-modal parameter spaces. The OE method assumes Gaussian distributed uncertain-

ties in the model parameters and uses gradient-descent optimization which is arguably less efficient in detecting global minima and sampling multi-modal spaces compared to Monte Carlo methods such as MCMC or Nested sampling. Nevertheless, the OE method has been used in the retrievals of several exoplanetary spectra to provide important constraints on their atmospheric properties. (Lee et al. 2012, 2014; Barstow et al. 2017).

Markov chain Monte Carlo (MCMC)

The MCMC method is one of the most widely used Bayesian inference methods in astronomy (Trotta 2017). In this method the exploration of the parameter space starts at an initial guess and progresses as a random walk wherein any given step in the "chain" depends only on the previous step. For example, in the commonly used Metropolis-Hastings algorithm the progression of the random walk is guided by the following procedure. At each step in the chain the decision to accept the next step is based on the ratio of the posteriors between the two steps. Consider a current step with parameter set θ_i giving the posterior $p(\theta_i|d)$. The parameter set for next step θ_{i+1} is drawn from a pre-specified distribution, such as a Gaussian centered on the current step with a pre-specified variance ("jump-length") for each parameter, and has a posterior $p(\theta_{i+1}|d)$. Then, step i+1 is accepted with a probability $p = \min(p(\theta_{i+1}|d)/p(\theta_i|d), 1)$ such that step i+1 is accepted if p is greater than a random number drawn from a uniform distribution between 0 and 1. The resulting full chain of steps through the parameter space essentially gives the joint posterior probability distribution of all the model parameters. More details on the MCMC method and variations thereof can be found in various works (Tegmark et al. 2004; Ford 2006; Line et al. 2013; Trotta 2017).

The MCMC method has been extensively used for exoplanetary atmospheric retrievals (Madhusudhan et al. 2011a; Benneke and Seager 2012; Line et al. 2013). The method allows efficient and extensive sampling of the posterior distribution, and allows the specification of prior distributions of the parameters where applicable. Generally for exoplanetary atmospheres there is usually very little prior knowledge. Therefore, retrievals typically allow for uniform priors with conservative ranges. Despite its capabilities, the MCMC method faces some limitations, especially for complex parameter spaces. For example, the MCMC method is not optimized for calculating the evidence $\mathscr{Z}$ which is computationally demanding. This is acceptable for parameter estimation of a given model, where $\mathscr{Z}$ acts as a normalization constant, but makes it challenging to conduct model comparisons when multiple models are plausible. Secondly, the MCMC method requires the user to specify the width of the distribution from which to draw each subsequent step, which is judged by trial and error and can effect convergence. These limitations are alleviated in the Nested Sampling method discussed below.

Nested Sampling

Recently, the Nested Sampling (NS) method has emerged as a powerful alternative to the MCMC method in Bayesian inference (Skilling 2006; Shaw et al. 2007; Feroz et al. 2009). As such, it has been promptly adopted in exoplanetary atmospheric retrieval codes (e.g., Benneke and Seager 2013; Line et al. 2015; Waldmann et al. 2015b; Lavie et al. 2017; MacDonald and Madhusudhan 2017a; Gandhi and Madhusudhan 2018). The NS method is also a Monte Carlo method like the MCMC but with a different approach to sample the parameter space. Instead of starting with an initial guess and following a Markov chain, as in MCMC, the NS method starts with a given number of "live points" in the parameter space randomly drawn from the prior distribution (Feroz et al. 2009). At each step the point with the lowest likelihood ($\mathscr{L}_{\rm min}$) is discarded and replaced by another point drawn from the prior distribution with $\mathscr{L} > \mathscr{L}_{\rm min}$, i.e. from the prior volume contained within the iso-likelihood contour of $\mathscr{L}_{\rm min}$. Thus, the live points are drawn from progressively shrinking ellipsoids bound by the iso-likelihood contours in subsequent trials. The process is repeated as the contours sweep through the parameter space and the evidence $\mathscr{Z}$ is calculated until a pre-set tolerance on the fractional change in $\mathscr{Z}$ is reached. The required tolerance ensures that convergence is naturally reached. Once the evidence is determined, the posterior distributions are computed based on all the points sampled in the parameter space over the entire optimization process.

The NS method has several advantages over other Bayesian inference methods. One of the main advantages of the NS method is that it is designed to be highly efficient for computing the Bayesian evidence ($\mathscr{Z}$) for a given model, which makes it particularly desirable when comparing between multiple models. In efficiently exploring the model parameter space to compute $\mathscr{Z}$ with high accuracy, the NS method also naturally allows high density sampling of the posterior distribution. This makes the NS method especially suited for handling complex model parameter spaces with multimodal and non-Gaussian posterior distributions. Secondly, the optimisation algorithm is naturally parallelised, thereby significantly reducing computation time. Finally, unlike MCMC, it does not require specification of the distribution from which to sample the parameters which would be required in each step of a Markov Chain.

Results

The retrieval methods described above have been used to retrieve chemical abundances, temperature profiles, and other atmospheric parameters for a number of exoplanets using different observational methods. Here we discuss the constraints reported in the literature for transiting planets observed via transmission and emission spectra as well as directly imaged planets in emission spectra.

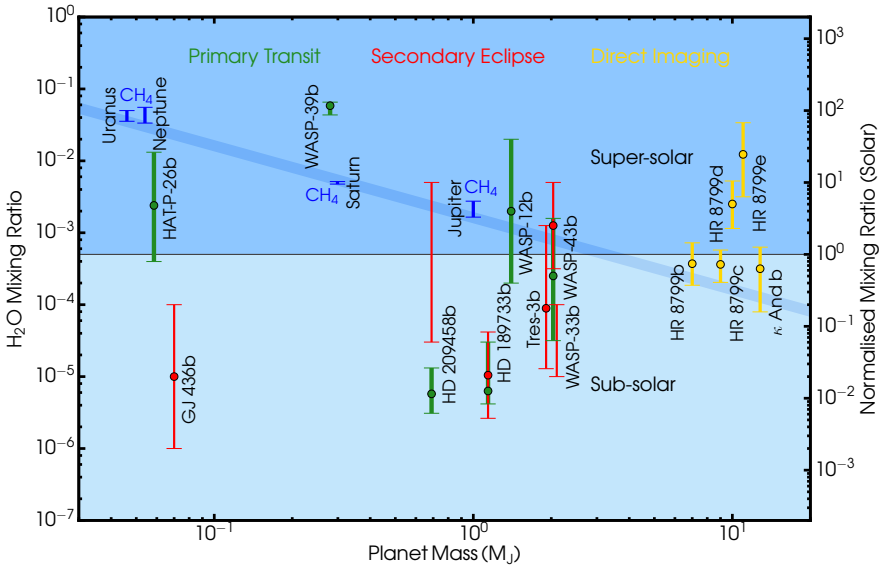

Fig. 3 Retrieved H_2O abundances for exoplanets in the literature with uncertainties in H_2O mixing ratios below 2 dex. The abundances derived from spectra obtained using different methods are colour-coded as shown at the top. Also shown (in blue) are the CH_4 abundances for the four solar system giant planets for which the H_2O abundances are not known. The solar system CH_4 abundances are obtained for Jupiter and Saturn from Atreya et al. (2016),Wong et al. (2004), and Fletcher et al. (2009), for Neptune from Karkoschka and Tomasko (2011), and for Uranus from Sromovsky et al. (2011). The exoplanet H_2O abundances are from the various works: HD 209458b (Madhusudhan et al. 2014a; MacDonald and Madhusudhan 2017a; Line et al. 2016), HD 189733b (Madhusudhan et al. 2014a; Waldmann et al. 2015a), WASP-12b (Kreidberg et al. 2015), WASP-43b (Kreidberg et al. 2014a), WASP-33b (Haynes et al. 2015), TrES-3 (Line et al. 2014), GJ 436b (Moses et al. 2013a), HAT-P-26b (Wakeford et al. 2017), WASP-39b (Wakeford et al. 2018), HR 8799 planets (Lavie et al. 2017), κ And b (Todorov et al. 2016).

Transmission spectra of transiting exoplanets

Most of the retrievals to date have been conducted on transmission spectra. A transmission spectrum probes the atmosphere at the day-night terminator region of a transiting exoplanet. The retrieved properties include chemical compositions, pressure-temperature (P-T) profiles, and cloud properties. In general, a transmission spectrum is less sensitive to detailed shape of the P-T profile but still provides a reasonable constraint on the representative photospheric temperature at the day-night terminator. On the other hand, the transmission spectrum is highly sensitive to the composition and presence of clouds/hazes. In what follows, we discuss published statistical constraints on atmospheric properties of exoplanets using retrievals of transmission spectra.

Key sources of data

Here we focus on reported high-precision transmission spectra with instruments whose systematics are well characterized and results reproducible. Datasets used in initial retrieval studies were limited by large uncertainties and/or underestimated systematics rendering the abundance determinations unreliable. The advent of the HST WFC3 spectrograph (McCullough and MacKenty 2012) has truly opened the era of high-precision abundance measurements from transmission spectra of exoplanets. The HST WFC3 G141 grism with its spectral range of 1.1-1.7 μm contains strong absorption features due to H_2O, along with other molecules (e.g. CH_4, NH_3, HCN). Additionally, the WFC3 instrument has proven to be highly stable and conducive to transit spectroscopy with demonstrated understanding of the systematics in numerous studies (e.g., Deming et al. 2013; Mandell et al. 2013; McCullough et al. 2014; Kreidberg et al. 2014b). Besides HST WFC3 in the near-infrared, the HST STIS spectrograph in the visible is sensitive to optical slopes of transmission spectra which in turn constrain sources of scattering (e.g. aerosols or molecular Rayleigh scattering) in the atmospheres (e.g., Pont et al. 2008, 2013; Sing et al. 2016; Wakeford and Sing 2015; Pinhas and Madhusudhan 2017). Other data sources used in retrievals include photometric data in the infrared obtained with the Spitzer Space Telescope typically at 3.6 μm and 4.5 μm (e.g., Fraine et al. 2014) as well as ground-based spectra/photometry in the visible and near-infrared (e.g., Sedaghati et al. 2017).

Reporting retrieved abundances

The retrieved chemical abundances are typically reported as volume mixing ratios (i.e. number density of a species relative to total or relative to H_2 which is the dominant species in giant planet atmospheres). It is also common to refer to the mixing ratios relative to "solar" values, i.e., those expected in thermochemical equilibrium at the relevant temperature (T) for an atmosphere with solar elemental abundances, O/H = 5×10^{-4}, C/H = 2.5×10^{-4}, C/O = 0.5 (Asplund et al. 2009). The portion of oxygen in H_2O in chemical equilibrium depends primarily on the overall metallicity, the C/O ratio, and the temperature and pressure (see e.g., Madhusudhan et al. 2016, for a detailed review on atmospheric chemistry). For solar abundance atmospheres with $T \sim$ 1200-3500 K and $\lesssim$1200 K, the typical value of solar H_2O/H_2 is 5×10^{-4} and $\sim 10^{-3}$, respectively, with the remaining oxygen locked in CO and other species. Reported H_2O abundances greater or lower than these values are referred to as super-solar or sub-solar H_2O, respectively.

Abundance estimates in hot Jupiters

The majority of retrieved abundances using HST WFC3 transmission spectra have been reported for H_2O in hot Jupiters, as shown in Fig. 3. The earliest high-precision

WFC3 transmission spectra were observed for the hot Jupiters HD 209458b (Deming et al. 2013) and HD 189733b (McCullough et al. 2014). Atmospheric retrievals of these spectra (Madhusudhan et al. 2014a) suggested sub-solar H_2O abundances in these hot Jupiters, assuming cloud-free atmospheres. Other notable examples of high-precision transmission retrievals include the hot Jupiters WASP-43b (Kreidberg et al. 2014b) and WASP-12b (Kreidberg et al. 2015) for which H_2O abundances between 0.1-3$\times$ solar have been derived. H_2O abundance estimates in giant exoplanets today are routinely achieving uncertainties below 1 dex, as shown in Fig. 3, which is a significant achievement considering that the true H_2O abundance is not known for any of the giant planets in the solar system owing to their low temperatures (Atreya et al. 2016; Madhusudhan et al. 2016).

The precision of an abundance estimate is directly related to the quality of the observed spectrum. In particular the two factors of an observed spectrum that affect critically are (a) the precision, and (b) the spectral range. In particular the availability of data spanning the visible (e.g. using HST STIS) to infrared (e.g. HST WFC3 and Spitzer) range is critical for accurate retrievals of transmission spectra. The best example is the visible-IR transmission spectrum of HD 209458b where the average precision on the data is $\sim$25 ppm in the WFC3 which led to an abundance estimate with an uncertainty of $\lesssim$ 0.5 dex (Madhusudhan et al. 2014a; Barstow et al. 2017; MacDonald and Madhusudhan 2017a). Such a dataset was feasible for HD 209458b considering that it orbits one of the brightest exoplanet host stars (V = 7.8 magnitude). Fainter host stars often require integration of multiple spectra to achieve similar precisions (Stevenson et al. 2014b; Kreidberg et al. 2014b). Thus, focused repeat observations with HST have the potential to yield high-precision abundance estimates in more giant exoplanets. The upcoming JWST will substantially revolutionise abundance determinations in exoplanet atmospheres with a much larger aperture and spectral range (Greene et al. 2016).

Beyond H_2O abundances, constraints on other atmospheric properties from retrievals of transmission spectra are relatively sparse. In recent years, thanks to the combination of near-infrared and optical spectra, there have been nominal constraints on the parameters of clouds/hazes in the atmospheres, such as cloud top pressure, optical slopes due to hazes, patchiness, Na/K, etc (Barstow et al. 2017; MacDonald and Madhusudhan 2017a). Recent retrievals are also suggesting the first indications of Nitrogen-based chemistry in the form of NH_3 and/or HCN (MacDonald and Madhusudhan 2017b). Other recent developments in transmission retrievals include the detection of TiO in the transmission spectrum of hot Jupiter WASP-19b (Sedaghati et al. 2017).

A recurring finding in the majority of transmission spectra of hot Jupiters is that the amplitudes of H_2O features in the spectra are significantly muted (e.g., Deming et al. 2013; McCullough et al. 2014; Mandell et al. 2013; Kreidberg et al. 2015). The features contain the equivalent of $\sim$2 atmospheric scale heights compared to 5-10 expected for a saturated molecular absorption feature (e.g. Madhusudhan and Redfield 2015). It has been argued that such muted features can be caused by either clouds/hazes in the atmospheres obstructing parts of the atmospheres from view (Deming et al. 2013; Sing et al. 2016) or due to inherently low H_2O abun-

dances in the atmospheres (Madhusudhan et al. 2014a). In a recent study Sing et al. (2016) reported broadband transmission spectra of ten hot Jupiters and, using a forward model grid, suggested that a diversity of clouds/hazes with solar or super-solar H_2O abundances could explain all the spectra. However, a subsequent retrieval study (Barstow et al. 2017) reported the contrary that almost all the hot Jupiters in the Sing et al. (2016) sample indicated sub-solar H_2O abundances, consistent with other retrieval studies (Madhusudhan et al. 2014a; MacDonald and Madhusudhan 2017a) for some of the planets. This demonstrates the importance of retrievals over traditional equilibrium models in deriving abundances. On the other hand, transmission retrievals of some hot Jupiters, e.g. WASP-43b and WASP-12b (Kreidberg et al. 2014a, 2015), while also consistent with sub-solar H_2O abundances have uncertainties large enough to allow somewhat super-solar abundances.

Abundance estimates in hot Neptunes and super-Earths

In recent years, we are beginning to witness detections of molecular features in transmission spectra of extrasolar ice giants, the so called hot Neptunes. Early HST WFC3 observations of hot Neptunes (e.g., GJ 436b, Knutson et al. 2014) and super-Earths (e.g., GJ 1214b, Kreidberg et al. 2014a) showed mostly flat transmission spectra. However, more recent observations of hot Neptunes HAT-P-11b (Fraine et al. 2014) and HAT-P-26b (Wakeford et al. 2017) have shown clear absorption features of H_2O at high significance. Retrievals of these spectra have reported abundances in terms of atmospheric metallicity with 1-σ constraints of $\sim$40-300$\times$ solar for HAT-P-11b and $\sim$1-26$\times$solar for HAT-P-26b. Note that here H_2O is assumed to be the primary carrier of oxygen whose abundance in turn is used to represent the metallicity. Besides these abundance constraints currently there is still a dearth of precise abundance constraints for hot Neptunes and super-Earths. The imminent arrival of JWST is expected to revolutionize abundance estimates in such low mass planets.

Thermal emission spectra of transiting exoplanets

Emission spectra of transiting exoplanets provide constraints on the properties of their dayside atmospheres. Unlike transmission spectra, emission spectra are strongly sensitive not only to the chemical composition but also to the *P-T* profile of the atmosphere. It is thermal emission directly from the planet that is measured and is strongly governed by the temperature distribution in the atmosphere. Emission measurements in one or more bands have been measured for over 50 exoplanets to date. However, in order to conduct detailed retrieval of the atmospheric properties, observations over a long spectral range are required. Such observations are available for $\lesssim$10 planets to date.

Thermal emission retrievals have provided key constraints on three properties of the dayside atmospheres of hot transiting exoplanets: molecular abundances, C/O ratios, and thermal inversions. The constraints have been reported mostly for hot Jupiters but also include one hot Neptune. The contributions of these properties in different observational bandpasses are discussed in several works (e.g. Burrows et al. 2008; Madhusudhan 2012; Madhusudhan et al. 2014b; Moses et al. 2013b; Mollière et al. 2017).

Molecular Abundances

The chemical abundances have been reported mainly for H_2O with broad constraints on a few other species such as CO, CO_2, and CH_4. Figure 3 shows the H_2O abundance constraints from various studies. The earliest abundance estimates in emission retrievals were based primarily on broadband Spitzer photometry (Madhusudhan and Seager 2009; Stevenson et al. 2010; Madhusudhan and Seager 2011; Lee et al. 2012; Line et al. 2013) and constrained molecular abundances with large uncertainties. Additionally, the most extensive Spitzer observations used in such retrievals, e.g. for hot Jupiters HD 189733b (Charbonneau et al. 2008) and HD 209458b (Knutson et al. 2008) have since been revised to very different values (e.g. Knutson et al. 2012; Diamond-Lowe et al. 2014) rendering the former abundances unreliable. The success of HST WFC3 and ground-based near-infrared photometry in recent years have led to more reliable constraints on H_2O abundances. Such reported H_2O abundances on the daysides of hot Jupiters include 0.4-3.5$\times$ solar in WASP-43b (Kreidberg et al. 2014b), $\lesssim$0.01$\times$ solar in WASP-12b (Madhusudhan et al. 2011a; Stevenson et al. 2014a), 0.06-10$\times$ solar in HD 209458b (Line et al. 2016), $\lesssim$ 0.2 $\times$ solar in WASP-33b (Haynes et al. 2015), among others.

The sum-total of abundance measurements convey two key findings. Firstly, with the combination of high-precision emission data from HST, Spitzer, and ground-based instruments we are now able to measure H_2O abundances with uncertainties to within an order of magnitude. Secondly, similar to transmission spectra, the abundance estimates from emission retrievals are also suggesting H_2O abundances lower than originally expected. The median values of the H_2O abundances for most of the planets reported to date are sub-solar, though the uncertainties allow between 0.1-3.5$\times$ solar values. Additionally, the incidence of clouds/hazes which are degenerate with the H_2O abundance determinations in transmission spectra is less of a problem in emission retrievals, given the much higher dayside temperatures and the fact that the spectrum probes the temperature profile and composition above a putative cloud deck if any.

Abundance retrievals for species other than H_2O are significantly less precise. Nevertheless, several retrieval studies have reported useful limits on carbon-bearing species with potentially interesting implications. For example, significantly super-solar abundances of CO and CO_2 have been reported in the hot Neptune GJ 436b suggesting strong non-equilibrium chemistry and high ($\gtrsim$ 10-30$\times$solar) overall

metallicity (Stevenson et al. 2010; Madhusudhan and Seager 2011; Lanotte et al. 2014).

C/O Ratios

An important development in emission retrievals is the feasibility of constraining C/O ratios in exoplanetary atmospheres. This was first demonstrated for the hot Jupiter WASP-12b using MCMC retrievals on a multi-band photometric dataset spanning a wide spectral range from 1-10 μm comprising Spitzer and ground-based photometry (Madhusudhan et al. 2011a). The retrieved abundances suggested low H_2O ($\lesssim$0.01$\times$ solar) and higher CO and CH_4 compared to H_2O leading to a C/O $\geq$ 1, which is significantly carbon-rich compared to the solar C/O of 0.54 with important implications (Madhusudhan et al. 2011b; Madhusudhan 2012). The claim of high C/O in WASP-12b has been contested in subsequent studies (e.g., Crossfield et al. 2012; Cowan et al. 2012) though a recent analysis considering newer Spitzer and HST observations reinstated the claim (Stevenson et al. 2014a), especially due to the non-detection of H_2O in the WFC3 emission spectrum. On the other hand, a transmission spectrum of the terminator shows a low-amplitude H_2O feature that is consistent with a oxygen-rich as well as a carbon-rich composition (Kreidberg et al. 2015). The dependance of H_2O abundance on the C/O ratio varies with temperature; for C/O = 1 the H_2O abundance is more strongly depleted at higher temperatures typical of dayside atmospheres (Madhusudhan 2012). Nevertheless, the C/O ratio of WASP-12b is currently still under debate, considering the limited data available, which can be resolved by future observations with the upcoming JWST.

The case of WASP-12b demonstrated the potential of thermal emission spectra to constrain C/O ratios in exoplanetary atmospheres. It is to be noted, however, that reliable constraints on C/O ratios are possible only when observations over a long spectral baseline are available with the observed bands containing spectral features from both H_2O as well as prominent carbon-bearing species such as CO and/or CH_4. This is ostensibly possible with the combination of spectra with HST WFC3 and the Spitzer IRAC bands between 3-8 μm. However, few systems have such extensive datasets. Using the limited datasets available, C/O ratios for several hot Jupiters have been reported to lie between 0.1-1 (Madhusudhan 2012; Line et al. 2014; Haynes et al. 2015; Kreidberg et al. 2014b; Line et al. 2016). On the other hand, when adequate data are not available and only H_2O abundances can be measured from HST WFC3, some studies have also attempted to infer the C/O ratio based on assumptions of thermochemical equilibrium (Kreidberg et al. 2015; Line et al. 2016). Overall, the C/O ratio has emerged to be a measurable quantity of high importance for future higher resolution spectroscopy, e.g., with JWST.

Thermal Inversions

Thermal emission spectra have also been instrumental in constraining temperature profiles in the dayside atmospheres of exoplanets. In particular, the search for thermal inversions in hot Jupiter atmospheres has been one of the most important pursuits in exoplanetary atmospheres in the past decade. The temperature gradient in the atmosphere along with the composition, through opacity, governs the amplitude of the spectral features. Whereas a temperature profile monotonically decreasing outward gives rise to absorption features, that increasing outward (i.e. a thermal inversion) gives rise to emission features. On the other hand, an isothermal atmosphere emits as a blackbody with the corresponding temperature. These features have been predicted using self-consistent models well before retrievals came into practice (e.g., Hubeny et al. 2003; Burrows et al. 2007; Fortney et al. 2008).

Retrievals of emission spectra of transiting hot Jupiters have revealed the diversity in their *P-T* profiles. Initial retrievals (Madhusudhan and Seager 2009, 2010) revealed the strong degeneracies between temperature profiles and compositions. Thanks to recent HST WFC3 spectra and ground-based photometry of thermal emission, strong constraints on temperature profiles have become possible for several transiting exoplanets. Most of these planets observed to date have been found to host no thermal inversions (Madhusudhan and Seager 2010; Line et al. 2013), some highlights being WASP-43b (Kreidberg et al. 2014b; Stevenson et al. 2014b), HD 209458b (Line et al. 2016), and WASP-12b (Madhusudhan et al. 2011a; Stevenson et al. 2014a). On the other hand, thermal inversions have been convincingly detected in three hot Jupiters: WASP-33b (Haynes et al. 2015), WASP-121b (Evans et al. 2017) and WASP-18b (Sheppard et al. 2017), which are amongst the most extremely irradiated hot Jupiters known, with equilibrium temperatures of $\sim$3000 K. Therefore, retrievals of emission spectra to date show that thermal inversions are prevalent in only the hottest of hot Jupiters at temperatures of $\sim$3000 K, much above the $\sim$1500 K boundary originally suggested by Fortney et al. (2008).

Thermal emission spectra of directly imaged planets

Retrievals of directly-imaged planets are still in their infancy considering the small number of such planets with atmospheric spectra. On the one hand, the spectra are typically of much higher quality than those currently available for transiting planets (Barman et al. 2011; Konopacky et al. 2013). On the other hand, direct imaging retrievals are more challenging compared to transiting planet retrievals because of the various unknowns and degeneracies. For example, for directly imaged planets only the emission spectrum of the planet is observed without much a priori information about several of the system parameters, e.g. radius, gravity/mass, any measure of temperature, distance to the system, etc. Therefore, all these quantities need to be set as free parameters in the retrievals. And, considering that these are typically young systems, the luminosity and radius of the planet are strongly dependent on

the age and can have a wide range(Burrows et al. 2001). Finally, given the low levels of irradiation, such planets have been known to host significantly dusty atmospheres (Marley et al. 2012) and convection playing a stronger role in the temperature profiles compared to transiting planets which are highly irradiated.

Some recent studies have made important advancements towards retrievals of directly imaged planets with important constraints on their atmospheric properties. Retrievals have been reported for the planets in the HR 8799 system (Lee et al. 2013; Lavie et al. 2017) and for the κ Andromedae b (Todorov et al. 2016), using different retrievals approaches: NEMESIS Optimal Estimation (Lee et al. 2013), MULTINEST Nested sampling (Lavie et al. 2017), and MCMC (Todorov et al. 2016). Lee et al. (2013) and Lavie et al. (2017) reported constraints on the abundances of the prominent molecules H_2O, CO, CH_4, and CO_2 in HR 8799b, with the later study also reporting constraints on a subset of the species in HR 8799c,d,e. Generally, the studies find super-solar abundances in all the species and super-solar C/O ratios ($\sim$0.75-0.96) for HR 8799b and c. And, Lavie et al. (2017) report sub-solar C/H and C/O and super-solar O/H for HR 8799 d and e. On the other hand, Todorov et al. (2016) report the H_2O abundance of κ Andromedae b to be nearly solar, albeit with a larger uncertainty. These studies demonstrate the high-precisions with which abundances can be retrieved for directly-imaged planets. On the other hand, the studies also reveal the challenges in such retrievals. For example, Lee et al. (2013) find too small radii for young giant planets (0.6-0.8) that are seemingly unphysical whereas Lavie et al. (2017) had to adopt a strong prior on the radii (1.2 ± 0.1 R_J), log(gravity) (4.1 ± 0.3), and distance (39.4 ± 1 pc) to facilitate the retrievals.

Challenges and Future Directions

Retrieval is an extremely powerful tool but also one to be used with due care. Inherent to Bayesian inference is the grand reality that in the limit of very poor data quality the posterior asymptotes to the prior. Therefore, arguably the best approach in retrieval is to allow the data to shepherd one to the reality of an atmosphere with as few model assumptions as absolutely necessary. On the other hand, the insufficient data quality means that one is tempted to recourse to arguments of physical/chemical plausibility to narrow down the solution space, leaving open the definition of plausibility in the unknown conditions of an exoplanetary atmosphere. Furthermore, given the highly complex, non-linear, and degenerate parameter space of atmospheric models, any statistical inference algorithm used must ensure to sample the parameter space rigorously and efficiently. The main limitation at the moment is the data quality, of a limited spectral range and precision, which is expected to greatly improve with the upcoming JWST and large ground-based facilities. In what follows, we discuss some key challenges faced in retrievals of exoplanetary spectra with current data in the hope that they serve as important lessons for the future.

Degeneracies in Abundance Estimates

The main challenge in abundance estimates using retrievals is the prevalence of strong degeneracies between different chemical species and among other atmospheric properties. Foremost among them is the degeneracy between clouds/hazes and abundances, particularly while retrieving transmission spectra. A low amplitude spectral feature can be caused either by clouds/hazes (Deming et al. 2013; Sing et al. 2016) or due to inherently low abundances (Madhusudhan et al. 2014a). Secondly, in transmission retrievals the abundances are also degenerate with the reference pressure corresponding to the quoted radius of the planet if spectra in only a limited infrared spectral range, such as HST WFC3, are available (Heng and Kitzmann 2017). Both these degeneracies can be resolved with high-precision spectra over a long spectral baseline, from visible to infrared, and with multiple molecular features, as demonstrated in some recent studies (Barstow et al. 2017; MacDonald and Madhusudhan 2017a). While such data are available only for a handful of planets currently, these examples highlight the critical importance of optical spectra along with infrared spectra in constraining molecular abundances.

Low-amplitude Spectral Features

One of the greatest surprises in transit spectroscopy in recent years is the ubiquitously low amplitudes in the spectra. As discussed in the results section, even for the hottest of hot Jupiters the spectra are surprisingly muted, amounting to $\lesssim$2 scale heights instead of 5-8 expected for a saturated absorption feature. This is seen in both transmission as well as emission spectra. The low amplitudes in transmission spectra could be due to clouds or low H_2O abundances. Retrievals of current broadband data with models including clouds/hazes still suggest sub-solar abundances as the favored explanation for hot Jupiters (Barstow et al. 2017; MacDonald and Madhusudhan 2017a) but it remains to be further investigated with future data. On the other hand, the low amplitudes in emission spectra could potentially be due to low temperature gradients or, again, low abundances. Whatever the present interpretation, the ground reality is that spectral observations and retrievals using future facilities such as JWST should be prepared for low amplitude spectral features in potentially most planets.

Biases in Estimating C/O ratios and Metallicities

When data are insufficient to constrain a certain quantity, retrievals sometimes invoke additional model assumptions to narrow down the solution space. While this could be useful to some extent to rule out extremely unphysical solutions, caution must be exercised on this path. For example, this is commonly seen in quoting

constraints on quantities such as the C/O ratio and metallicities (Kreidberg et al. 2015; Line et al. 2016; Wakeford et al. 2017) when only HST WFC3 data are available with constraints on only the H_2O abundance. Retrievers then assume chemical equilibrium, amongst other factors, to estimate which C/O ratios could cause the retrieved H_2O abundances for the retrieved *P-T* profiles; the process is sometimes termed "chemically consistent retrievals". Similarly, H_2O is often used as a proxy for metallicity by inherently assuming a certain C/O ratio. At the extreme end of this trend, inferences of metallicities are sometimes made solely using equilibrium forward models, i.e., without retrievals (Sing et al. 2016), only to find contrasting conclusions when retrievals are performed later on the same datasets (Barstow et al. 2017). Whereas Sing et al. (2016) claimed none of the ten planets in their survey were consistent with sub-solar H_2O, Barstow et al. (2017) reported that all the planets were consistent with sub-solar H_2O. Therefore, care must be taken against using such inferences of C/O ratios or metallicities with equilibrium assumptions as a true measure of the atmospheric composition since various non-equilibrium effects are unaccounted for in the process. Ultimately, the most reliable estimates are those that are obtained from retrievals with minimal model assumptions and guided by high-fidelity datasets.

New Trends and Future Prospects

New advancements in retrievals are being made in several directions. With increasing data quality there is increasing sophistication in the forward models used in retrievals. One development in this direction is the consideration of two-dimensional effects, such as multiple P-T profiles (Feng et al. 2016) and inhomogeneous cloud cover(Line and Parmentier 2016; MacDonald and Madhusudhan 2017a). Secondly, we are also seeing the emergence of "hybrid" codes where retrievals are fully interfaced with self-consistent equilibrium models to place constraints on disequilibrium phenomena, such as departures from radiative-convective and thermochemical equilibria (Gandhi and Madhusudhan 2018). Thirdly, on the observational side, a major development is the idea of combining low-resolution transit spectroscopy with very high resolution ($R\sim10^5$) ground-based spectroscopy(Brogi et al. 2017). The latter method, which is essentially doppler spectroscopy of molecular lines in the planetary atmosphere, has in recent years proved to be the most effective technique for conclusive detections of molecular species in exoplanetary atmospheres (Snellen et al. 2010; Brogi et al. 2012; Birkby et al. 2017). Combining this method with traditional transit spectroscopy provides a new avenue for high-fidelity atmospheric retrievals. There have also been efforts to try machine learning techniques such as artificial neural networks for retrievals (Waldmann 2016) but their efficacy on real datasets and benefits over state-of-the-art Bayesian inference methods remains to be seen.

We are at the beginning of a revolution in atmospheric characterization of exoplanets. Atmospheric retrievals today are equipped with state-of-the-art Bayesian

inference techniques combined with detailed forward models and are limited only by current data quality. The latter is going to change very soon with the imminent arrival of JWST and ramping up of ground-based spectroscopy with large facilities. JWST will have a broad spectral range ($\sim$0.6-25 μm), high spectral resolution and precision. These capabilities will allow detection of a wide range of species besides H_2O, such as CO, CO_2, CH_4, NH_3, and others, and precise determinations of their abundances (Greene et al. 2016), along with constraints on the *P-T* profiles, aerosols forming clouds/hazes, energy budget, etc. These constraints in turn will allow us to understand a wide range of atmospheric processes such as non-equilibrium chemistry, thermal inversions, atmospheric dynamics, cloud formation, etc. The molecular abundances will also allow precise constraints on the C/H, O/H, C/O, and other elemental abundance ratios, which will be instrumental in constraining planetary formation conditions (see e.g. review by Madhusudhan et al. 2016). And, finally, atmospheric retrievals of low mass planets could pave the way to the first detections of biosignatures epitomizing the holy grail of the exoplanetary science.

Acknowledgements The author acknowledges the tireless efforts by various groups working on exoplanetary atmospheric retrieval which has led to the exponential rise in this area in the last eight years. The author thanks A. Pinhas for help with Table 1 and Fig. 3, A. Pinhas and R. MacDonald for help with references, and L. Welbanks for help with Fig. 2. The author thanks the chapter editor Sara Seager for very helpful comments.

References

Asplund M, Grevesse N, Sauval AJ Scott P (2009) The Chemical Composition of the Sun. ARA&A47:481–522

Atreya SK, Crida A, Guillot T et al. (2016) The Origin and Evolution of Saturn, with Exoplanet Perspective. ArXiv e-prints

Barman T (2007) Identification of Absorption Features in an Extrasolar Planet Atmosphere. ApJ661:L191–L194

Barman TS, Macintosh B, Konopacky QM Marois C (2011) Clouds and Chemistry in the Atmosphere of Extrasolar Planet HR8799b. ApJ733:65

Barstow JK, Aigrain S, Irwin PGJ Sing DK (2017) A Consistent Retrieval Analysis of 10 Hot Jupiters Observed in Transmission. ApJ834:50

Benneke B Seager S (2012) Atmospheric Retrieval for Super-Earths: Uniquely Constraining the Atmospheric Composition with Transmission Spectroscopy. ApJ753:100

Benneke B Seager S (2013) How to Distinguish between Cloudy Mini-Neptunes and Water/Volatile-dominated Super-Earths. ApJ778:153

Bétrémieux Y Kaltenegger L (2015) Refraction in planetary atmospheres: improved analytical expressions and comparison with a new ray-tracing algorithm. MNRAS451:1268–1283

Birkby JL, de Kok RJ, Brogi M, Schwarz H Snellen IAG (2017) Discovery of Water at High Spectral Resolution in the Atmosphere of 51 Peg b. AJ153:138

Blecic P (2015) Observations, Thermochemical Calculations, and Modeling of Exoplanetary Atmospheres. PhD thesis, University of Central Florida

Brogi M, Snellen IAG, de Kok RJ et al. (2012) The signature of orbital motion from the dayside of the planet τ Boötis b. Nature486:502–504

Brogi M, Line M, Bean J, Désert JM Schwarz H (2017) A Framework to Combine Low- and High-resolution Spectroscopy for the Atmospheres of Transiting Exoplanets. ApJ839:L2

Brown TM (2001) Transmission Spectra as Diagnostics of Extrasolar Giant Planet Atmospheres. ApJ553:1006–1026

Burrows A, Hubbard WB, Lunine JI Liebert J (2001) The theory of brown dwarfs and extrasolar giant planets. Reviews of Modern Physics 73:719–765

Burrows A, Hubeny I, Budaj J, Knutson HA Charbonneau D (2007) Theoretical Spectral Models of the Planet HD 209458b with a Thermal Inversion and Water Emission Bands. ApJ668:L171–L174

Burrows A, Budaj J Hubeny I (2008) Theoretical Spectra and Light Curves of Close-in Extrasolar Giant Planets and Comparison with Data. ApJ678:1436-1457

Charbonneau D, Knutson HA, Barman T et al. (2008) The Broadband Infrared Emission Spectrum of the Exoplanet HD 189733b. ApJ686:1341-1348

Cowan NB, Machalek P, Croll B et al. (2012) Thermal Phase Variations of WASP-12b: Defying Predictions. ApJ747:82

Crossfield IJM, Barman T, Hansen BMS, Tanaka I Kodama T (2012) Re-evaluating WASP-12b: Strong Emission at 2.315 μm, Deeper Occultations, and an Isothermal Atmosphere. ApJ760:140

Cubillos P (2015) In Pursuit of New Worlds: Searches for and Studies of Transiting Exoplanets from Three Space-Based Observatories. PhD thesis, University of Central Florida

de Wit J (2015) Maps and Masses of Transiting Exoplanets: Towards New Insights into Atmospheric and Interior Properties of Planets. ArXiv e-prints

Deming D, Wilkins A, McCullough P et al. (2013) Infrared Transmission Spectroscopy of the Exoplanets HD 209458b and XO-1b Using the Wide Field Camera-3 on the Hubble Space Telescope. ApJ774:95

Diamond-Lowe H, Stevenson KB, Bean JL, Line MR Fortney JJ (2014) New Analysis Indicates No Thermal Inversion in the Atmosphere of HD 209458b. ApJ796:66

Eastman J, Gaudi BS Agol E (2013) EXOFAST: A Fast Exoplanetary Fitting Suite in IDL. PASP125:83

Evans TM, Sing DK, Kataria T et al. (2017) An ultrahot gas-giant exoplanet with a stratosphere. Nature548:58–61

Feng YK, Line MR, Fortney JJ et al. (2016) The Impact of Non-uniform Thermal Structure on the Interpretation of Exoplanet Emission Spectra. ApJ829:52

Feroz F, Hobson MP Bridges M (2009) MULTINEST: an efficient and robust Bayesian inference tool for cosmology and particle physics. MNRAS398:1601–1614

Fletcher LN, Orton GS, Teanby NA, Irwin PGJ Bjoraker GL (2009) Methane and its isotopologues on Saturn from Cassini/CIRS observations. Icarus199:351–367

Ford EB (2005) Quantifying the Uncertainty in the Orbits of Extrasolar Planets. AJ129:1706–1717

Ford EB (2006) Improving the Efficiency of Markov Chain Monte Carlo for Analyzing the Orbits of Extrasolar Planets. ApJ642:505–522

Fortney JJ, Lodders K, Marley MS Freedman RS (2008) A Unified Theory for the Atmospheres of the Hot and Very Hot Jupiters: Two Classes of Irradiated Atmospheres. ApJ678:1419-1435

Fortney JJ, Shabram M, Showman AP et al. (2010) Transmission Spectra of Three-Dimensional Hot Jupiter Model Atmospheres. ApJ709:1396–1406

Fraine J, Deming D, Benneke B et al. (2014) Water vapour absorption in the clear atmosphere of a Neptune-sized exoplanet. Nature513:526–529

Gandhi S Madhusudhan N (2017) GENESIS: New Self-Consistent Models of Exoplanetary Spectra. ArXiv e-prints

Gandhi S Madhusudhan N (2018) Retrieval of exoplanet emission spectra with HyDRA. MNRAS474:271–288

Greene TP, Line MR, Montero C et al. (2016) Characterizing Transiting Exoplanet Atmospheres with JWST. ApJ817:17

Grillmair CJ, Burrows A, Charbonneau D et al. (2008) Strong water absorption in the dayside emission spectrum of the planet HD189733b. Nature456:767–769

Guillot T (2010) On the radiative equilibrium of irradiated planetary atmospheres. A&A520:A27
Haynes K, Mandell AM, Madhusudhan N, Deming D Knutson H (2015) Spectroscopic Evidence for a Temperature Inversion in the Dayside Atmosphere of Hot Jupiter WASP-33b. ApJ806:146
Heng K Kitzmann D (2017) The theory of transmission spectra revisited: a semi-analytical method for interpreting WFC3 data and an unresolved challenge. MNRAS470:2972–2981
Heng K Marley M (2017) Radiative Transfer for Exoplanet Atmospheres. ArXiv e-prints
Hubbard WB, Fortney JJ, Lunine JI et al. (2001) Theory of Extrasolar Giant Planet Transits. ApJ560:413–419
Hubeny I, Burrows A Sudarsky D (2003) A Possible Bifurcation in Atmospheres of Strongly Irradiated Stars and Planets. ApJ594:1011–1018
Irwin PGJ, Teanby NA, de Kok R et al. (2008) The NEMESIS planetary atmosphere radiative transfer and retrieval tool. J Quant Spectr Rad Transf109:1136–1150
Karkoschka E Tomasko MG (2011) The haze and methane distributions on Neptune from HST-STIS spectroscopy. Icarus211:780–797
Knutson HA, Charbonneau D, Allen LE, Burrows A Megeath ST (2008) The 3.6-8.0 μm Broadband Emission Spectrum of HD 209458b: Evidence for an Atmospheric Temperature Inversion. ApJ673:526-531
Knutson HA, Charbonneau D, Burrows A, O'Donovan FT Mandushev G (2009) Detection of A Temperature Inversion in the Broadband Infrared Emission Spectrum of TrES-4. ApJ691:866–874
Knutson HA, Lewis N, Fortney JJ et al. (2012) 3.6 and 4.5 μm Phase Curves and Evidence for Non-equilibrium Chemistry in the Atmosphere of Extrasolar Planet HD 189733b. ApJ754:22
Knutson HA, Benneke B, Deming D Homeier D (2014) A featureless transmission spectrum for the Neptune-mass exoplanet GJ436b. Nature505:66–68
Konopacky QM, Barman TS, Macintosh BA Marois C (2013) Detection of Carbon Monoxide and Water Absorption Lines in an Exoplanet Atmosphere. Science 339:1398–1401
Kreidberg L, Bean JL, Désert JM et al. (2014a) Clouds in the atmosphere of the super-Earth exoplanet GJ1214b. Nature505:69–72
Kreidberg L, Bean JL, Désert JM et al. (2014b) A Precise Water Abundance Measurement for the Hot Jupiter WASP-43b. ApJ793:L27
Kreidberg L, Line MR, Bean JL et al. (2015) A Detection of Water in the Transmission Spectrum of the Hot Jupiter WASP-12b and Implications for Its Atmospheric Composition. ApJ814:66
Lanotte AA, Gillon M, Demory BO et al. (2014) A global analysis of Spitzer and new HARPS data confirms the loneliness and metal-richness of GJ 436 b. A&A572:A73
Lavie B, Mendonça JM, Mordasini C et al. (2017) HELIOS-RETRIEVAL: An Open-source, Nested Sampling Atmospheric Retrieval Code; Application to the HR 8799 Exoplanets and Inferred Constraints for Planet Formation. AJ154:91
Lecavelier Des Etangs A, Pont F, Vidal-Madjar A Sing D (2008) Rayleigh scattering in the transit spectrum of HD 189733b. A&A481:L83–L86
Lee JM, Fletcher LN Irwin PGJ (2012) Optimal estimation retrievals of the atmospheric structure and composition of HD 189733b from secondary eclipse spectroscopy. MNRAS420:170–182
Lee JM, Heng K Irwin PGJ (2013) Atmospheric Retrieval Analysis of the Directly Imaged Exoplanet HR 8799b. ApJ778:97
Lee JM, Irwin PGJ, Fletcher LN, Heng K Barstow JK (2014) Constraining the Atmospheric Composition of the Day-Night Terminators of HD 189733b: Atmospheric Retrieval with Aerosols. ApJ789:14
Line MR Parmentier V (2016) The Influence of Nonuniform Cloud Cover on Transit Transmission Spectra. ApJ820:78
Line MR, Zhang X, Vasisht G et al. (2012) Information Content of Exoplanetary Transit Spectra: An Initial Look. ApJ749:93
Line MR, Wolf AS, Zhang X et al. (2013) A Systematic Retrieval Analysis of Secondary Eclipse Spectra. I. A Comparison of Atmospheric Retrieval Techniques. ApJ775:137
Line MR, Knutson H, Wolf AS Yung YL (2014) A Systematic Retrieval Analysis of Secondary Eclipse Spectra. II. A Uniform Analysis of Nine Planets and their C to O Ratios. ApJ783:70

Line MR, Teske J, Burningham B, Fortney JJ Marley MS (2015) Uniform Atmospheric Retrieval Analysis of Ultracool Dwarfs. I. Characterizing Benchmarks, Gl 570D and HD 3651B. ApJ807:183

Line MR, Stevenson KB, Bean J et al. (2016) No Thermal Inversion and a Solar Water Abundance for the Hot Jupiter HD 209458b from HST/WFC3 Spectroscopy. AJ152:203

Lupu RE, Marley MS, Lewis N et al. (2016) Developing Atmospheric Retrieval Methods for Direct Imaging Spectroscopy of Gas Giants in Reflected Light. I. Methane Abundances and Basic Cloud Properties. AJ152:217

MacDonald RJ Madhusudhan N (2017a) HD 209458b in new light: evidence of nitrogen chemistry, patchy clouds and sub-solar water. MNRAS469:1979–1996

MacDonald RJ Madhusudhan N (2017b) Signatures of Nitrogen Chemistry in Hot Jupiter Atmospheres. ApJ850:L15

Madhusudhan N (2012) C/O Ratio as a Dimension for Characterizing Exoplanetary Atmospheres. ApJ758:36

Madhusudhan N Redfield S (2015) Optimal measures for characterizing water-rich super-Earths. International Journal of Astrobiology 14:177–189

Madhusudhan N Seager S (2009) A Temperature and Abundance Retrieval Method for Exoplanet Atmospheres. ApJ707:24–39

Madhusudhan N Seager S (2010) On the Inference of Thermal Inversions in Hot Jupiter Atmospheres. ApJ725:261–274

Madhusudhan N Seager S (2011) High Metallicity and Non-equilibrium Chemistry in the Dayside Atmosphere of hot-Neptune GJ 436b. ApJ729:41

Madhusudhan N, Harrington J, Stevenson KB et al. (2011a) A high C/O ratio and weak thermal inversion in the atmosphere of exoplanet WASP-12b. Nature469:64–67

Madhusudhan N, Mousis O, Johnson TV Lunine JI (2011b) Carbon-rich Giant Planets: Atmospheric Chemistry, Thermal Inversions, Spectra, and Formation Conditions. ApJ743:191

Madhusudhan N, Crouzet N, McCullough PR, Deming D Hedges C (2014a) H_2O Abundances in the Atmospheres of Three Hot Jupiters. ApJ791:L9

Madhusudhan N, Knutson H, Fortney JJ Barman T (2014b) Exoplanetary Atmospheres. Protostars and Planets VI pp 739–762

Madhusudhan N, Agúndez M, Moses JI Hu Y (2016) Exoplanetary Atmospheres - Chemistry, Formation Conditions, and Habitability. Space Sci Rev 205:285–348

Mandell AM, Haynes K, Sinukoff E et al. (2013) Exoplanet Transit Spectroscopy Using WFC3: WASP-12 b, WASP-17 b, and WASP-19 b. ApJ779:128

Marley MS, Saumon D, Cushing M et al. (2012) Masses, Radii, and Cloud Properties of the HR 8799 Planets. ApJ754:135

McCullough P MacKenty J (2012) Considerations for using Spatial Scans with WFC3. Tech. rep.

McCullough PR, Crouzet N, Deming D Madhusudhan N (2014) Water Vapor in the Spectrum of the Extrasolar Planet HD 189733b. I. The Transit. ApJ791:55

Miller-Ricci E, Seager S Sasselov D (2009) The Atmospheric Signatures of Super-Earths: How to Distinguish Between Hydrogen-Rich and Hydrogen-Poor Atmospheres. ApJ690:1056–1067

Mollière P, van Boekel R, Bouwman J et al. (2017) Observing transiting planets with JWST. Prime targets and their synthetic spectral observations. A&A600:A10

Moses JI, Line MR, Visscher C et al. (2013a) Compositional Diversity in the Atmospheres of Hot Neptunes, with Application to GJ 436b. ApJ777:34

Moses JI, Madhusudhan N, Visscher C Freedman RS (2013b) Chemical Consequences of the C/O Ratio on Hot Jupiters: Examples from WASP-12b, CoRoT-2b, XO-1b, and HD 189733b. ApJ763:25

Oreshenko M, Lavie B, Grimm SL et al. (2017) Retrieval Analysis of the Emission Spectrum of WASP-12b: Sensitivity of Outcomes to Prior Assumptions and Implications for Formation History. ApJ847:L3

Pinhas A Madhusudhan N (2017) On Signatures of Clouds in Exoplanetary Transit Spectra. ArXiv e-prints

Pont F, Knutson H, Gilliland RL, Moutou C Charbonneau D (2008) Detection of atmospheric haze on an extrasolar planet: the 0.55-1.05 μm transmission spectrum of HD 189733b with the HubbleSpaceTelescope. MNRAS385:109–118

Pont F, Sing DK, Gibson NP et al. (2013) The prevalence of dust on the exoplanet HD 189733b from Hubble and Spitzer observations. MNRAS432:2917–2944

Robinson TD (2017) A Theory of Exoplanet Transits with Light Scattering. ApJ836:236

Rodgers CD (2000) Inverse Methods for Atmospheric Sounding - Theory and Practice. Inverse Methods for Atmospheric Sounding - Theory and Practice Series: Series on Atmospheric Oceanic and Planetary Physics, ISBN: ¡ISBN¿9789812813718¡/ISBN¿ World Scientific Publishing Co Pte Ltd, Edited by Clive D Rodgers, vol 2 2

Seager S (2010) Exoplanet Atmospheres: Physical Processes

Seager S Sasselov DD (2000) Theoretical Transmission Spectra during Extrasolar Giant Planet Transits. ApJ537:916–921

Sedaghati E, Boffin HMJ, MacDonald RJ et al. (2017) Detection of titanium oxide in the atmosphere of a hot Jupiter. Nature549:238–241

Shaw JR, Bridges M Hobson MP (2007) Efficient Bayesian inference for multimodal problems in cosmology. MNRAS378:1365–1370

Sheppard KB, Mandell AM, Tamburo P et al. (2017) Evidence for a Dayside Thermal Inversion and High Metallicity for the Hot Jupiter WASP-18b. ApJ850:L32

Sing DK, Fortney JJ, Nikolov N et al. (2016) A continuum from clear to cloudy hot-Jupiter exoplanets without primordial water depletion. Nature529:59–62

Skilling J (2006) Nested sampling for general bayesian computation. Bayesian Anal 1(4):833–859, URL http://dx.doi.org/10.1214/06-BA127

Snellen IAG, de Kok RJ, de Mooij EJW Albrecht S (2010) The orbital motion, absolute mass and high-altitude winds of exoplanet HD209458b. Nature465:1049–1051

Sromovsky LA, Fry PM Kim JH (2011) Methane on Uranus: The case for a compact CH $_4$ cloud layer at low latitudes and a severe CH $_4$ depletion at high-latitudes based on re-analysis of Voyager occultation measurements and STIS spectroscopy. Icarus215:292–312

Stevenson KB, Harrington J, Nymeyer S et al. (2010) Possible thermochemical disequilibrium in the atmosphere of the exoplanet GJ 436b. Nature464:1161–1164

Stevenson KB, Bean JL, Madhusudhan N Harrington J (2014a) Deciphering the Atmospheric Composition of WASP-12b: A Comprehensive Analysis of its Dayside Emission. ApJ791:36

Stevenson KB, Désert JM, Line MR et al. (2014b) Thermal structure of an exoplanet atmosphere from phase-resolved emission spectroscopy. Science 346:838–841

Swain MR, Vasisht G Tinetti G (2008) The presence of methane in the atmosphere of an extrasolar planet. Nature452:329–331

Tegmark M, Strauss MA, Blanton MR et al. (2004) Cosmological parameters from SDSS and WMAP. Phys Rev D69(10):103501

Tegmark M, Eisenstein DJ, Strauss MA et al. (2006) Cosmological constraints from the SDSS luminous red galaxies. Phys Rev D74(12):123507

Tinetti G, Vidal-Madjar A, Liang MC et al. (2007) Water vapour in the atmosphere of a transiting extrasolar planet. Nature448:169–171

Todorov KO, Line MR, Pineda JE et al. (2016) The Water Abundance of the Directly Imaged Substellar Companion κ And b Retrieved from a Near Infrared Spectrum. ApJ823:14

Trotta R (2017) Bayesian Methods in Cosmology. ArXiv e-prints

Wakeford HR Sing DK (2015) Transmission spectral properties of clouds for hot Jupiter exoplanets. A&A573:A122

Wakeford HR, Sing DK, Kataria T et al. (2017) HAT-P-26b: A Neptune-mass exoplanet with a well-constrained heavy element abundance. Science 356:628–631

Wakeford HR, Sing DK, Deming D et al. (2018) The Complete Transmission Spectrum of WASP-39b with a Precise Water Constraint. AJ155:29

Waldmann IP (2016) Dreaming of Atmospheres. ApJ820:107

Waldmann IP, Rocchetto M, Tinetti G et al. (2015a) Tau-REx II: Retrieval of Emission Spectra. ApJ813:13

Waldmann IP, Tinetti G, Rocchetto M et al. (2015b) Tau-REx I: A Next Generation Retrieval Code for Exoplanetary Atmospheres. ApJ802:107

Wong MH, Mahaffy PR, Atreya SK, Niemann HB Owen TC (2004) Updated Galileo probe mass spectrometer measurements of carbon, oxygen, nitrogen, and sulfur on Jupiter. Icarus171:153–170